

Study on Active Particle Doped Fluorescent Fiber Temperature Sensing Technology

Jinling Wu¹, Hualong Yu² and Xiaowei Li³

¹*Institute of Occupation Technical, Hebei Normal University, Shijiazhuang, China*

²*Institute of Education, Hebei Normal University, Shijiazhuang, China*

³*Shijiazhuang Municipal Public Security Bureau, Shijiazhuang, China*

Keywords: Visible wavelength; absorbing glass; fluorescence optic sensor

Abstract: The optic- fiber temperature measurement probe based on ruby is developed. This system is particularly adapt to the temperature measurement in the rang of 0°C to 130°. The calibration graph was shown to be highly reproducible when the probe is temperature cycled. A change in drive current from 5 to 30mA yields a spectral shift of the peak emission of only a few nanometers. The drive current to the LED can easily be kept within the required narrowly defined bounds through the control circuitry.

1 INTRODUCTION

The previous device was configured to take advantage of infrared radiation and the infrared absorption characteristics in the sensor. Such a scheme is, in principle, attractive as a reference for any absorption-based device, but may be limited by its operation with infrared radiation. Many processes involve interactions in the visible part of the spectrum, e. g., pH indicator dyes and colorimetric processes, and with the availability of bright LED and laser diode sources in the visible part of the spectrum, there is a genuine need for such a referencing scheme at shorter wavelengths into the visible. Furthermore, in the device described, the sensitivity of the resultant sensor was somewhat limited and did offer scope for potential improvement. One such method is to consider the suitability of visible wavelength referencing system for temperature sensors

2 OPTICAL AND MECHANICAL DESIGN

In this case the temperature-dependent absorbing material is a sample of glass, which exhibits a significant change in its optical properties, on a band centered at 565nm, the emission wavelength of the commonly available bright green LED. Crystal ruby

is used as the material producing the reference fluorescence signal. On the R-line emission bands, don't discuss here.

The ruby and absorbing glass sample that constituted the sensor probe was held together in a metal cylinder of length 25mm, using large diameter input and output optical fibers (PCS1000, 1000μm diameter). At the wavelength of the ruby fluorescence, the absorbing glass has maximum transmission and this is sufficiently removed spectrally not to change significantly with temperature, up to ~1300C. Beyond this temperature an unacceptable (>1%) deviation in the otherwise constant fluorescence ratio occurs and thus the ruby sample can only be used for referencing when mounted in a different configuration, in front of the LED. This is well below the temperature where catastrophic chemical changes occur in the glass (several hundred degrees Celsius), and its absorption properties change irreversibly.

3 SIGNAL PROCESSING SCHEME

A block diagram of the system, which was designed to separate, in time, the changes in the temperature-dependent green light and the fluorescence reference red light signals, is shown in Figure 1. where systems 1 and 2 refer to two different placements of the ruby sample in order to optimize the

performance of the device. In system1, the ruby sample is in contact with the absorbing glass and in system2 it is located in front of the LED, in a standard optical housing. The LED was modulated with a pulse, which falls to zero on a time scale of several Microseconds and thus the signal received after this time corresponds to the total ruby Fluorescence signal caused by excitation of the sample by the green light.

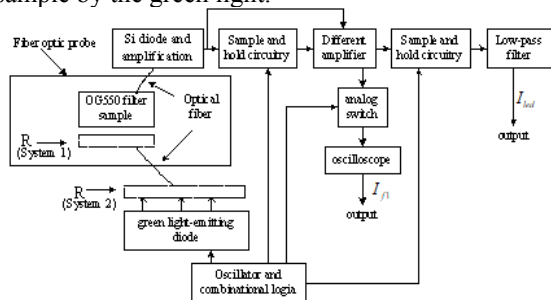


Figure 1. Block diagram of the optoelectronic system.

Thus, a single detector may be used, in this case a Si p-i-n diode with an integral amplifier, to amplify the low signal levels experienced. This obviates the need for two such detectors to separate each wavelength band and any consequent difficulty that may occur in their cross referencing. To



Figure 2. The illustration of transmitted intensity of the green LED signal, and time-integrated ruby fluorescence, showing temporal Division of signals. Horizontal time scale-5ms div-1.

eliminate the effect of ambient light variations, a sample/hold circuit samples the signal when the LED is off and also where the fluorescence signal has decayed to its zero level. The sampled value is then subtracted from the original signal in a difference amplifier and as a consequence the signal is referred to level independent of ambient light variations. It is then processed in two different ways.

The temperature-dependent signal is obtained by sampling the pulse at its maximum value and a first-order low-pass filter to minimize fluctuations due to noise further smooths the corresponding dc output. The 'reference' signal is obtained by electronically switching out only the fluorescence signal.

Typical pulses from which this information was obtained are shown as Figure2, illustrating intensities of the transmitted green signal from the LED, and the ruby fluorescence pulse of time-integrated intensity.

4 SYSTEM PERFORMANCE

4.1 Validity of the Referencing Technique with Ruby

The time-integrated fluorescence signal obtained from the ruby sample must be a direct measure of the intensity of the green LED signal which both induces it and is attenuated in a temperature-dependent way by the absorbing glass sample Figure3.

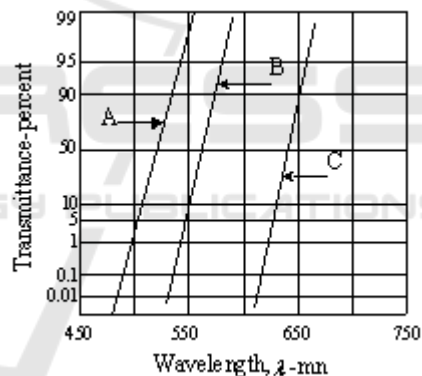


Figure 3. Transmittance (at room temperature) of three Absorption glasses OG515 (A), OG550 (B), RG630(C).

Shows the proof of this principle, where the ratio of the peak green LED signal obtained under steady pumping, to the time-integrated fluorescence, is shown as a function of temperature for a probe made up with only the ruby present and the absorption of the glass. Over the range 20-1300C, the ratio is constant to $\pm 1\%$ of the peak value, clearly showing validity of the referencing technique, as would Be expected from the constant quantum efficiency of the ruby. It is important to carry out such a test as the geometrical changes in the probe itself can mean significant changes in the intensity of the green signal reaching the absorbing glass.

Beyond 130, this does not apply to required degree of accuracy, thus dictating the only probe design, which may then be used, excluding system 1 in favor of system 2, in the temperature region to 200°C.

4.2 Choice of Absorbing Material

Three absorption edge glasses were tested initially with the ruby sample housed in front of the LED. Figure 4 shows a series of absorption spectra at room temperature, of the three filters OG515(A), OG550(B), and RG630(C), with, for comparison, the emission profile of the green LED(L). The calibration graph of the normalized transmission of these three materials as a function of temperature in the range 20-130°C is shown as Figure 8.16. Over this range, for OG515(A), the maximum change in intensity is ± 1.5%, which is due essentially to the error in the ruby referencing and noise in the system. The result indicates OG515 is too far removed from the LED spectrum to make any real impression on the transmitted intensity. The calibration graph with RG 630(C), shows a slightly nonlinear profile of normalized transmission with temperature. The change in the ratio recorded on this graph was 25% over the temperature range studied. From the LED profile in Figure 4 it can be seen that main absorption of RG630 is well beyond the peak wavelength of the LED. Thus, the percentage change in transmitted intensity in the probe itself can be improved by using a glass whose characteristic is optimum near the center wavelength. OG550 (B), with 45% transmission at 550nm, shows a 45% change in intensity over the same temperature range. As a result this type glass was chosen for the sensor system investigated.

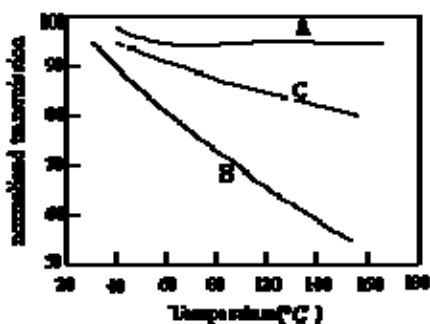


Figure 4. Normalized transmission as a function of temperature of three absorption glasses (20~300C), A, B, C.

4.3 Calibration Graphs

The normalized transmission factor is plotted as a function of temperature and is shown in Figure 5 (A), and (B), for a probe-containing ruby and with the ruby directly in front of the LED. A slightly nonlinear response results with the experimental points closely following the smooth response curve. A small deviation of the system 1 graph (A) occurs as the normalized transmission decreases due to the small decrease in the signal/noise ratio. Up to the 130°C limit. For system 2, the smooth function continues up to the maximum temperature of study, 200°C.

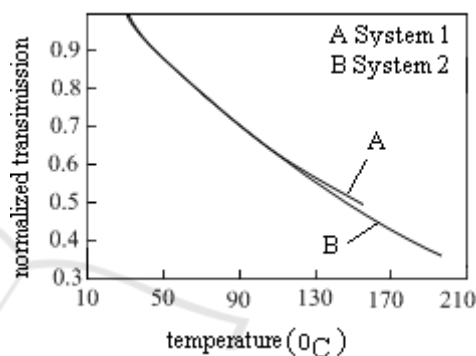


Figure 5. Normalized transmission of probe as a function of temperature.

5 CONCLUSIONS

A considerably improved performance is seen in this new device over that discussed using infrared radiation. The slope of the calibration graph from that work was $1.7 \times 10^{-3} \text{K}^{-1}$ and thus it can be seen that the visible radiation-based device is more sensitive, with a slope, 75°C of $4.1 \times 10^{-3} \text{K}^{-1}$. The standard deviation of the typical reading was measured as 0.11°C. Hence, the temperature accuracy of this reading is ± 0.6°C using the 'best-fit' curve drawn on Figure 5. The calibration graph was shown to be highly reproducible when the probe is temperature cycled. Drift of the device is low and problems of LED ageing will not be significant if the diode is not severely overrun in terms of the applied current. A change in drive current from 5 to 30mA yields a spectral shift of the peak emission of only a few nanometers. As the ruby absorption bands are broad this will cause only a negligible change in the fluorescent intensity of emission and the effect on the determination of the absorption profile of the OG550 glass will also be very small. The drive current to the

LED can easily be kept within the required narrowly defined bounds through the control circuitry.

ACKNOWLEDGEMENTS

This project is supported by the Key project of Hebei Provincial Department of Education (No.ZD2016040) ; This project is supported by Hebei science and technology research item(No.12201708D); The project is supported by Hebei Normal Universty application fund (No.L2015k09).

REFERENCES

1. XiaXiang, JianbinShi, FenghongHuang, Mingming Zheng, Qianchun Deng. Quantum dots-based label-free fluorescence sensor for sensitive and non-enzymatic detection of caffeic acid. *Talanta*, Volume 141, 15 August 2015, Pages 182-187.
2. Tae-Jin Kim, Kyung-A Kim, Sang Hoon Jung. Development of an endoplasmic reticulum calcium sensor based on fluorescence resonance energy transfer. *Sensors and Actuators B: Chemical*, Volume 247, August 2017, Pages 520-525.
3. Florent Lefèvre, Philippe Juneau, Ricardo Izquierdo. Integration of fluorescence sensors using organic optoelectronic components for microfluidic platform. *Sensors and Actuators B: Chemical*, Volume 221, 31 December 2015, Pages 1314-1320.
4. Chunlei Yang, Wenping Deng, Haiyun Liu, Shenguang Ge, Mei Yan. Turn-on fluorescence sensor for glutathione in aqueous solutions using carbon dots-MnO₂ nanocomposites. *Sensors and Actuators B: Chemical*, Volume 216, September 2015, Pages 286-292.
5. Hong zhi Lu, Shoufang Xu. Visualizing BPA by molecularly imprinted ratiometric fluorescence sensor based on dual emission nanoparticles. *Biosensors and Bioelectronics*, Volume 92, 15 June 2017, Pages 147-153.